INTERNATIONAL JOURNAL OF NUMERICAL MODELLING : ELECTRONIC NETWORKS, DEVICES AND FIELDS,
Vol. 10, 177–192 (1997)

OPTIMIZED ENTIRE-DOMAIN MOMENT-METHOD ANALYSIS OF 3D DIELECTRIC SCATTERERS

B. M. NOTAROŠ AND B. D. POPOVIĆ*

Department of Electrical Engineering, University of Belgrade, P.O. Box 35–54, 11120 Belgrade, Yugoslavia

SUMMARY

When compared with commonly used subdomain moment-method analysis, entire-domain analysis of 3D dielectric scatterers results in a greatly reduced number of unknowns. Unfortunately, the expressions for matrix elements tend to be quite complicated and their calculation extremely time-consuming if evaluated directly. It is shown in the paper that, in a Galerkin-type solution with large trilinear hexahedral basic volume elements and three-dimensional polynomial approximation of volume current inside them, these expressions can be manipulated analytically for optimized rapid non-redundant integration. Consequently, a method for the analysis of 3D dielectric scatterers is obtained that is efficient, rapidly converging with increasing degree of approximation for current, remarkably accurate and very moderate in computer memory requirements. The applicability of the method of moments is thereby extended to bodies of electrical sizes greatly exceeding those that can be dealt with by subdomain methods. © 1997 by John Wiley & Sons, Ltd.

Int. J. Numer. Model., **10**, 177–192 (1997)

No. of Figures: 8. No. of Tables: 3. No. of References: 10.

1. INTRODUCTION

The moment-method numerical analysis of 3D dielectric scatterers is one of the most challenging electromagnetic problems. The principal difficulty is a very large number of unknowns involved in such an analysis. On one hand, this requires computers of large storage capabilities. On the other hand, solution for the unknowns is a very time-consuming procedure.

This paper deals with the analysis of 3D dielectric scatterers based on the solution of the volume integral equation for current (or field) distribution. The existing methods for the solution of this equation are of subdomain type. Consequently, basis functions of low order (3D pulse functions or 3D rooftop functions) are used for the approximation of unknown generalized current distribution inside electrically small volume elements (cubes, parallelepipeds or tetrahedrons).[1–3] This results in relatively simple evaluation of the system matrix elements, but in a prohibitively large number of unknowns for even electrically medium-sized problems. Although there are subdomain methods which possess the convolution structure of the solution and use the conjugate gradient FFT technique to speed up the computation,[3] the large number of unknowns nevertheless limits their applicability severely.

One way of reducing the number of unknowns is to use entire-domain basis functions inside volume elements much larger than in the subdomain approach. As far as the authors are informed, such a method has been used for the analysis of 3D dielectric scatterers in one reference only,[4] probably because of analytically quite complex and computationally time-consuming evaluation of the system matrix elements.

This present paper is aimed at demonstrating that the entire-domain approach can be optimized so that, with considerable reduction in both the total number of unknowns and the CPU time per unknown, the moment method becomes a powerful tool for analysis of 3D dielectric scatterers. The optimized method consists of four principal steps:

*Correspondence to: B. D. Popović, Department of Electrical Engineering, University of Belgrade, PO Box 35–54, 11120 Belgrade, Yugoslavia.

CCC 0894–3370/97/030177–16$17.50

Received 19 July 1996
Revised 6 November 1996

1. adoption of large trilinear hexahedrons as elements for the approximation of the scatterer geometry[5]
2. approximation of volume currents by simple and flexible entire-domain 3D polynomials in local parametric co-ordinates (generally not orthogonal) inside these elements
3. adoption of the Galerkin method for numerical solution of the volume integral equation, and specific transformations of the Galerkin generalized impedances (the system matrix elements) which enable their efficient numerical evaluation, and
4. extensive analytical manipulations and careful programming (discussed in great detail in the paper) in order to minimize the time necessary for the evaluation of the system matrix elements (i.e. generalized impedances).

An accurate method for the analysis of 3D dielectric scatterers is thus obtained which, on average, results in at least an order of magnitude fewer unknowns, and consequently very much reduced total CPU time, when compared with the existing, subdomain, methods. The method appears to converge rapidly with the increasing degree of polynomial approximation and to be remarkably stable. The applicability of the moment-method solutions of 3D dielectric scatterers is thereby greatly extended. For example, problems which would otherwise require very large computers can be solved efficiently on normal-size personal computers.

2. GENERALIZED IMPEDANCES IN THE GALERKIN SOLUTION OF THE VOLUME INTEGRAL EQUATION FOR CURRENT INSIDE TRILINEAR HEXAHEDRONS

2.1. *Generalized Galerkin impedances for arbitrary volume elements*

Imagine first an arbitrary inhomogeneous scatterer, possibly lossy, situated in a vacuum in an incident electromagnetic field. Let the scatterer be made of a linear dielectric or permittivity ϵ, conductivity σ and permeability μ_0, and let the angular frequency of the incident wave be ω. We solve for volume currents in the scatterer starting from the volume integral equation and the method of moments.[6]

Assume first that the scatterer is approximated by a number of arbitrary volume elements. Let us approximate the complex total (polarization plus conduction) induced current-density vector, $\mathbf{J}$, inside them by convenient functional series with unknown complex coefficients. The generalized impedances (the system matrix elements) are then given by[6]

$$Z_{mn} = \int_{V_m} \mathbf{J}_m \cdot \mathbf{E}_n \, \mathrm{d}V_m \tag{1}$$

where $\mathbf{J}_m$ represents arbitrary testing (weighting) function inside the mth element, of volume V_m, and $\mathbf{E}_n$ the electric-field vector due to the current component corresponding to arbitrary basis function $\mathbf{J}_n$ in the nth element. If $n = m$, a term $\Delta Z_{mn} = -\int[\mathrm{j}\omega(\epsilon_n - \epsilon_0) + \sigma_n]^{-1} \, \mathbf{J}_m \cdot \mathbf{J}_n \, \mathrm{d}V_m$ must be added to Z_{mn}, but its evaluation is trivial, and we shall not consider it here. For the same reason we shall not consider the elements of the free-terms (excitation) column matrix of the system of linear equations (known as generalized voltages[6]). Finally, we adopt the Galerkin testing method, i.e. the same testing and basis functions.

The vector $\mathbf{E}_n$ can be evaluated as follows:

$$\mathbf{E}_n = -\mathrm{j}\omega\mathbf{A}_n - \mathrm{grad}\Phi_n \tag{2}$$

$$\mathbf{A}_n = \mu_0 \int_{V_n} \mathbf{J}_n g(\mathbf{r}_m,\mathbf{r}_n) \, \mathrm{d}V_n \tag{3}$$

$$\Phi_n = \frac{1}{\epsilon_0}\left[\int_{V_n} \rho_n \, g(\mathbf{r}_m,\mathbf{r}_n) \, \mathrm{d}V_n + \oint_{S_n} \rho_{sn} \, g(\mathbf{r}_m,\mathbf{r}_n) \, \mathrm{d}S_n\right] \tag{4}$$

$$\rho_n = \frac{j}{\omega} \mathrm{div}\, \mathbf{J}_n, \quad \rho_{sn} = -\frac{j}{\omega} \mathbf{i}_{sn} \cdot \mathbf{J}_n \tag{5}$$

In these equations, $\mathbf{A}$ and Φ are the Lorentz potentials, ρ and ρ_s are densities of total (polarization plus free) induced volume and surface charges, S_n is the surface of the nth element, and $\mathbf{i}_{sn}$ is the outward unit vector normal to S_n. Finally, g is the free-space Green function,

$$g(\mathbf{r}_m,\mathbf{r}_n) = g(R) = \frac{e^{-j\beta_0 R}}{4\pi R}, \; R = |\mathbf{R}|, \; \mathbf{R} = \mathbf{r}_m - \mathbf{r}_n, \; \beta_0 = \omega\sqrt{(\epsilon_0\mu_0)} = \frac{2\pi}{\lambda_0} \tag{6}$$

where $\mathbf{r}_m$ and $\mathbf{r}_n$ are position vectors of the field point (inside the mth element) and the source point (inside the nth element), respectively.

Note that, if testing functions are well-behaved, $\mathbf{J}_m \cdot \text{grad}\Phi_n = \text{div}(\mathbf{J}_m\Phi_n) - \Phi_n \, \text{div}\mathbf{J}_m$. Using the divergence theorem and the above equations, the impedances Z_{mn} can be expressed as

$$Z_{mn} = -j\omega \left[\int_{V_m} (\mathbf{J}_m \cdot \mathbf{A}_n + \rho_m\Phi_n) \, dV_m + \oint_{S_m} \rho_{sm}\Phi_n \, dS_m \right] \tag{7}$$

where ρ_m and ρ_{sm} are given in (5), if all subscripts n are replaced by m.

2.2. *Trilinear hexahedral volume elements*

Let us now assume that the basic element of the geometrical model is the trilinear hexahedron,[5] sketched in Figure 1. This is a body defined by

$$\mathbf{r}(u,v,w) = \mathbf{r}_c + \mathbf{r}_u u + \mathbf{r}_v v + \mathbf{r}_w w + \mathbf{r}_{uv} uv + \mathbf{r}_{uw} uw + \mathbf{r}_{vw} vw + \mathbf{r}_{uvw} uvw, \quad u_1 \le u \le u_2, \; v_1 \le v \le v_2, \; w_1 \le w \le w_2 \tag{8}$$

where $\mathbf{r}$ is the position vector of a point inside the hexahedron with respect to the global origin, O, and u, v and w are arbitrary local co-ordinates. The parameters (u_1,u_2), (v_1,v_2) and (w_1,w_2) are local co-ordinates defining the hexahedron sides, and $\mathbf{r}_c$, $\mathbf{r}_u$, $\mathbf{r}_v$, $\mathbf{r}_w$, $\mathbf{r}_{uv}$, $\mathbf{r}_{uw}$, $\mathbf{r}_{vw}$ and $\mathbf{r}_{uvw}$ are constant vectors, that can be expressed in terms of the position vectors of the hexahedron vertices, $\mathbf{r}_{111}$, $\mathbf{r}_{112}$, ..., $\mathbf{r}_{222}$. Evidently, the hexahedron is defined uniquely by its eight vertices alone, which can be positioned in space arbitrarily. Except in special cases, the parametric u-v-w co-ordinate system is not orthogonal, and u, v and w are not length co-ordinates. All the trilinear hexahedron edges, as well as all co-ordinate lines, are straight.

The sides of a trilinear hexahedron are known as bilinear quadrilaterals,[7] which are generally inflexed. They coincide with co-ordinate surfaces. A bilinear quadrilateral is defined uniquely by

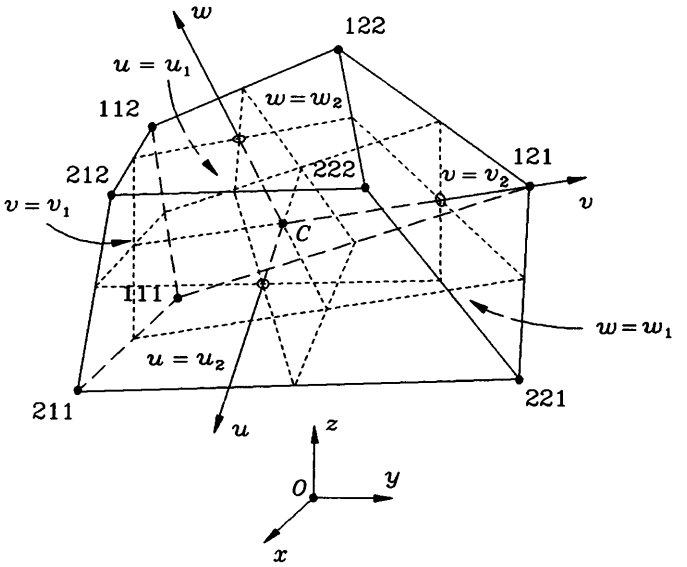

Figure 1. A trilinear hexahedron

its four vertices, which can be positioned arbitrarily. A typical bilinear quadrilateral is sketched in Figure 2.

Finally, a differential volume element at a point (u,v,w) of the trilinear hexahedron in Figure 1 is given by

$$\mathrm{d}V = K\,\mathrm{d}u\mathrm{d}v\mathrm{d}w,\ K = K(u,v,w) = \left(\frac{\partial \mathbf{r}}{\partial u} \times \frac{\partial \mathbf{r}}{\partial v}\right) \cdot \frac{\partial \mathbf{r}}{\partial w} \tag{9}$$

If we adopt the current-density vector in the form

$$\mathbf{J} = J_u \mathbf{i}_u + J_v \mathbf{i}_v + J_w \mathbf{i}_w = K^{-1}\left(J_u' \frac{\partial \mathbf{r}}{\partial u} + J_v' \frac{\partial \mathbf{r}}{\partial v} + J_w' \frac{\partial \mathbf{r}}{\partial w}\right) \tag{10}$$

where $\mathbf{i}_u = (\partial \mathbf{r}/\partial u)/|\partial \mathbf{r}/\partial u|$, $\mathbf{i}_v = (\partial \mathbf{r}/\partial v)/|\partial \mathbf{r}/\partial v|$ and $\mathbf{i}_w = (\partial \mathbf{r}/\partial w)/|\partial \mathbf{r}/\partial w|$ are unit vectors of the local u-v-w co-ordinate system, and J_u', J_v' and J_w' are normalized unknown current-density vector components, we can eliminate the function $K(u,v,w)$ from the integrals. After simple, but relatively lengthy, derivations, (3)–(10) result in the following Galerkin generalized impedance corresponding to the u-components of the vector $\mathbf{J}$ in the mth and nth volume elements:

$$Z_{mn}^{(u,u)} = -\,\mathrm{j}\omega \int_{u_{1m}}^{u_{2m}} \int_{v_{1m}}^{v_{2m}} \int_{w_{1m}}^{w_{2m}} \left(J_u' \frac{\partial \mathbf{r}}{\partial u}\right)_m \cdot \mathbf{A}_n^{(u)}\,\mathrm{d}u_m\,\mathrm{d}v_m\,\mathrm{d}w_m$$
$$+ \int_{u_{1m}}^{u_{2m}} \int_{v_{1m}}^{v_{2m}} \int_{w_{1m}}^{w_{2m}} \frac{\partial J_{um}'}{\partial u_m} \Phi_n^{(u)}\,\mathrm{d}u_m\,\mathrm{d}v_m\,\mathrm{d}w_m + \sum_{p=1}^{2} (-1)^{p-1} \int_{v_{1m}}^{v_{2m}} \int_{w_{1m}}^{w_{2m}} J_{um}'\big|_{u=u_{pm}} \Phi_n^{(u)}\,\mathrm{d}v_m\,\mathrm{d}w_m \tag{11}$$

where

$$\mathbf{A}_n^{(u)} = \mu_0 \int_{u_{1n}}^{u_{2n}} \int_{v_{1n}}^{v_{2n}} \int_{w_{1n}}^{w_{2n}} \left(J_u' \frac{\partial \mathbf{r}}{\partial u}\right)_n g(\mathbf{r}_m,\mathbf{r}_n)\,\mathrm{d}u_n\,\mathrm{d}v_n\,\mathrm{d}w_n \tag{12}$$

$$\Phi_n^{(u)} = \frac{\mathrm{j}}{\omega\epsilon_0}\left[\int_{u_{1n}}^{u_{2n}} \int_{v_{1n}}^{v_{2n}} \int_{w_{1n}}^{w_{2n}} \frac{\partial J_{un}'}{\partial u_n} g(\mathbf{r}_m,\mathbf{r}_n)\,\mathrm{d}u_n\,\mathrm{d}v_n\,\mathrm{d}w_n\right.$$
$$\left. + \sum_{l=1}^{2} (-1)^{l-1} \int_{v_{1n}}^{v_{2n}} \int_{w_{1n}}^{w_{2n}} [J_{un}'\, g(\mathbf{r}_m,\mathbf{r}_n)]\Big|_{u=u_{ln}} \mathrm{d}v_n\,\mathrm{d}w_n\right] \tag{13}$$

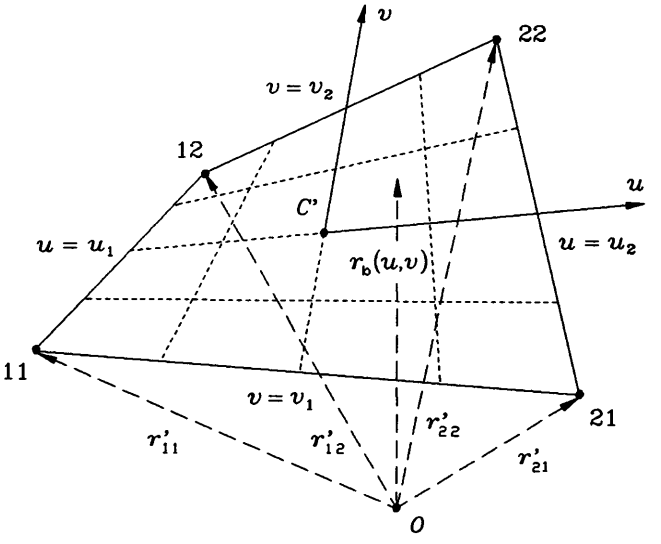

Figure 2. A bilinear quadrilateral

The vectors $\mathbf{r}_m$ and $\mathbf{r}_n$ are given in (8).

The above expression for the Galerkin generalized impedances and the potentials is very convenient for the following reasons:

1. It is valid for extremely flexible volume elements, trilinear hexahedrons (Figure 1), very simple to define (by eight points in space only), of any shape and electrical size, and interconnected arbitrarily.
2. The current-density vector is represented in terms of three local components, as opposed to four components necessary for (electrically small) tetrahedrons.[1]
3. The expressions have the same form as in the case of much simpler parallelepipedal elements of side lengths $u_2 - u_1$, $v_2 - v_1$ and $w_2 - w_1$, where the vector $\mathbf{J}'$ is decomposed in local orthogonal co-ordinates into rectangular components J'_u, J'_v and J'_w. The function K in (9) is a kind of Jakobian for mapping the trilinear hexahedron with current density $\mathbf{J}$ into a rectangular parallelepiped with normalized current density $\mathbf{J}'$. Therefore we shall refer to the expressions in (11)–(13) as the normalized generalized impedances and potentials.
4. The expressions contain only potentials, which, in turn, contain the weakest singularity possible, of the form $1/R$. This is very convenient for numerical integration of the integrals. In addition, no numerical differentiation is necessary (the term gradΦ is absent).

2.3. *Entire-domain polynomial approximation of current*

For the approximation of the components of the normalized current-density vector we adopt three-dimensional polynomials in the local co-ordinates,

$$J'_u = \sum_{i=0}^{N_u} \sum_{j=0}^{N_v} \sum_{k=0}^{N_w} a_{uijk}\, u^i v^j w^k, \begin{Bmatrix} u_1 \le u \le u_2 \\ v_1 \le v \le v_2 \\ w_1 \le w \le w_2 \end{Bmatrix} \tag{14}$$

and similarly for J'_v and J'_w. In this expansion, a_{uijk}, a_{vijk} and a_{wijk} are unknown coefficients to be determined, and N_u, N_v and N_w are the adopted degrees of the polynomials (the same for all three components of the current density in a hexahedron). The reason for the adoption of the polynomials as basis functions is their simplicity and high flexibility. The simplicity enables their rapid numerical evaluation. The flexibility makes it possible to approximate with reasonable accuracy very different functions in three variables with only few terms of the three-dimensional power series. As a consequence, trilinear hexahedrons need not be small, except where dictated by the scatterer geometry. In addition, the hexahedrons may be of (continuously) inhomogeneous dielectric.

For a single term in a component of the current density vector of the form $a_{uijk}u^i v^j w^k$ the potentials take the form

$$A_{ijk} = \mu_0\, a_{uijk} \left(\mathbf{r}_u P_{ijk} + \mathbf{r}_{uv} P_{i,j+1,k} + \mathbf{r}_{uw} P_{i,j,k+1} + \mathbf{r}_{uvw} P_{i,j+1,k+1} \right) \tag{15}$$

$$\Phi_{ijk} = \frac{j}{\omega \epsilon_0}\, a_{uijk} \left[i\, P_{i-1,j,k} + \sum_{l=1}^{2} (-1)^{l-1}\, u_l^i\, Q_{jk}^{(l)} \right] \tag{16}$$

In these equations, P_{ijk} is an integral over the volume of the trilinear hexahedron considered,

$$P_{ijk} = \int_{u_1}^{u_2} \int_{v_1}^{v_2} \int_{w_1}^{w_2} u^i v^j w^k\, g(\mathbf{r}_M, \mathbf{r})\, du dv dw \tag{17}$$

and $Q_{jk}^{(l)}$ is an integral over the side of the hexahedron defined by $u = u_l$ ($l = 1,2$):

$$Q_{jk}^{(l)} = \int_{v_1}^{v_2} \int_{w_1}^{w_2} v^j w^k\, g(\mathbf{r}_M, \mathbf{r}) \Big|_{u=u_l} dv dw \tag{18}$$

The vector $\mathbf{r}_M$ represents the (fixed) position vector of arbitrary field point M. In the Green function, g, defined in (6), the distance R is given by

$$R^2 = R^2(u,v,w) = [\mathbf{r}_M - \mathbf{r}(u,v,w)] \cdot [\mathbf{r}_M - \mathbf{r}(u,v,w)] \tag{19}$$

where $\mathbf{r}(u,v,w)$ is given by the parametric equation (8) of the hexahedron. It is a simple matter to prove that $R^2(u,v,w)$ can be expressed as

$$R^2(w) = a_1 w^2 + 2 a_2 w + a_3 \tag{20}$$

$$a_p(v) = b_{p1} v^2 + 2 b_{p2} v + b_{p3},\ p = 1,2,3 \tag{21}$$

$$b_{pq}(u) = c_{pq1} u^2 + 2 c_{pq2} u + c_{pq3},\ p = 1,2,3,\ q = 1,2,3 \tag{22}$$

where the constants c_{pqt} can be expressed in terms of the vectors $\mathbf{r}_M$, $\mathbf{r}_c$, ..., $\mathbf{r}_{uvw}$ (for example, $c_{111} = \mathbf{r}_{uvw} \cdot \mathbf{r}_{uvw}$).

From (14)–(16) and (8) it follows that the Galerkin generalized impedance, $Z_{mn}^{(u,u)}$ in (11), can be represented as a linear combination of four basic types of integral. These are the 3D/3D and 2D/2D Galerkin integrals,

$$S_{i_m j_m k_m i_n j_n k_n} = \int_{u_{1m}}^{u_{2m}} \int_{v_{1m}}^{v_{2m}} \int_{w_{1m}}^{w_{2m}} u_m^{i_m} v_m^{j_m} w_m^{k_m} P_{i_n j_n k_n}(\mathbf{r}_m)\, \mathrm{d}u_m\, \mathrm{d}v_m\, \mathrm{d}w_m \tag{23}$$

$$T_{j_m k_m j_n k_n}^{(p,l)} = \int_{v_{1m}}^{v_{2m}} \int_{w_{1m}}^{w_{2m}} v_m^{j_m} w_m^{k_m} Q_{j_n k_n}^{(l)}(\mathbf{r}_m|_{u_m = u_{pm}})\, \mathrm{d}v_m\, \mathrm{d}w_m \tag{24}$$

as well as the corresponding 3D/2D and 2D/3D integrals. The vector $\mathbf{r}_m$ is the position vector of a point of the mth trilinear hexahedron with co-ordinates u_m, v_m and w_m.

2.4. *Non-redundant evaluation of the S integrals*

The integrals that need to be evaluated in implementing the proposed method are both numerous and complicated multiple integrals that can be evaluated only numerically. Therefore it is imperative for an efficient solution to avoid any redundant operation in evaluating the integrals.

Of all the integrals, the most time-consuming evaluation is that of the S integrals in (23). The indicated 3D integration is over the domain of the mth hexahedron, while the 3D integration implicit in the P integral in (17) is over the domain of the nth hexahedron. Note, however, that the co-ordinates u, v and w, as well as the corresponding subscripts, in the integrals S and P are cyclic. Therefore, for a given pair of hexahedrons, the same sequence of the S integrals (for all the required values of the subscripts i_m, j_m, k_m, i_n, j_n and k_n) can be used also for the evaluation of the generalized impedances relating to the v- and w-components of the vector $\mathbf{J}$ in the two hexahedrons considered. In addition, the same sequence of the S integrals can be used in those 3D/3D parts of the impedances in (11) which contain either the potential $\mathbf{A}$ or the potential Φ.

Having this in mind, the algorithm has been constructed in which, for any hexahedron pair, first and only once, the entire sequence of the basic Galerkin integrals S is evaluated. These integrals are then introduced into all impedances containing them. Such an algorithm is extremely convenient, because there are nine combinations for the impedances, $Z_{mn}^{(u,u)}$, $Z_{mn}^{(u,v)}$, ..., $Z_{mn}^{(w,w)}$, and in all of them it is necessary to evaluate $\mathbf{A}$ and Φ. It is faster for an order of magnitude over that in which the impedances are evaluated without this procedure.

Finally, it is necessary to devise an efficient and accurate integration procedure for the basic potential integrals. This is dealt with in the next Section.

3. INTEGRATION OF THE BASIC POTENTIAL INTEGRALS

Consider a trilinear hexahedron and assume that we wish to evaluate the integral P_{ijk} in (17) at a point M defined by the position vector $\mathbf{r}_M$. The point M (the field point) may be inside the

hexahedron or on its surface, as in Figure 3(a), or outside the hexahedron, as in Figure 3(b). It is assumed that the source point inside the hexahedron, M', is defined by the position vector $\mathbf{r}$. In the Green function, g, of the integral P_{ijk}, the distance between M and M', R, is defined in (6), with the vector $\mathbf{r}$ defined in (8). Let $d = R_{\min}$, and denote by $M_0(u_0,v_0,w_0)$ the source point nearest to the field point, M. Of course, in the case of Figure 3(a), we have $M_0 \equiv M$ and $d = 0$.

When the distance d is relatively small (with respect to the dimensions of the hexahedron), the extraction of singularity [in the case of Figure 3(a)] or quasisingularity [in the case of Figure 3(b)] is performed. The principal, (quasi)singular, part of the integrand kernel of the P_{ijk} integral, for $R \approx 0$, is the function $1/R$. Unfortunately, analytical solution of the integral $\int (1/R)\, dV$ over the domain of an arbitrary trilinear hexahedron does not seem to exist. Consequently, in extracting the (quasi)singularity we shall integrate $1/R$ over the domain of a (generally not rectangular) parallelepiped, the sides of which are obtained by translating the straight segments A_1A_2, B_1B_2 and C_1C_2 shown in Figures 3(a) and 3(b). The parallelepipeds which correspond to the cases in Figures 3(a) and 3(b), are shown in Figures 3(c) and 3(d), respectively. Note that the co-ordinate segments A_1A_2, B_1B_2 and C_1C_2 are common for the trilinear hexahedron and the parallelepiped. For u close to u_0, v close to v_0 and w close to w_0, the point $M'(u,v,w)$ of the trilinear hexahedron coincides with, or is very close to, the point $M'_p(u,v,w)$ of the parallelepiped. Thus, in extracting the (quasi)singularity in the P_{ijk} integral we subtract and add a term of the form $1/R_p$ (instead of the form $1/R$),

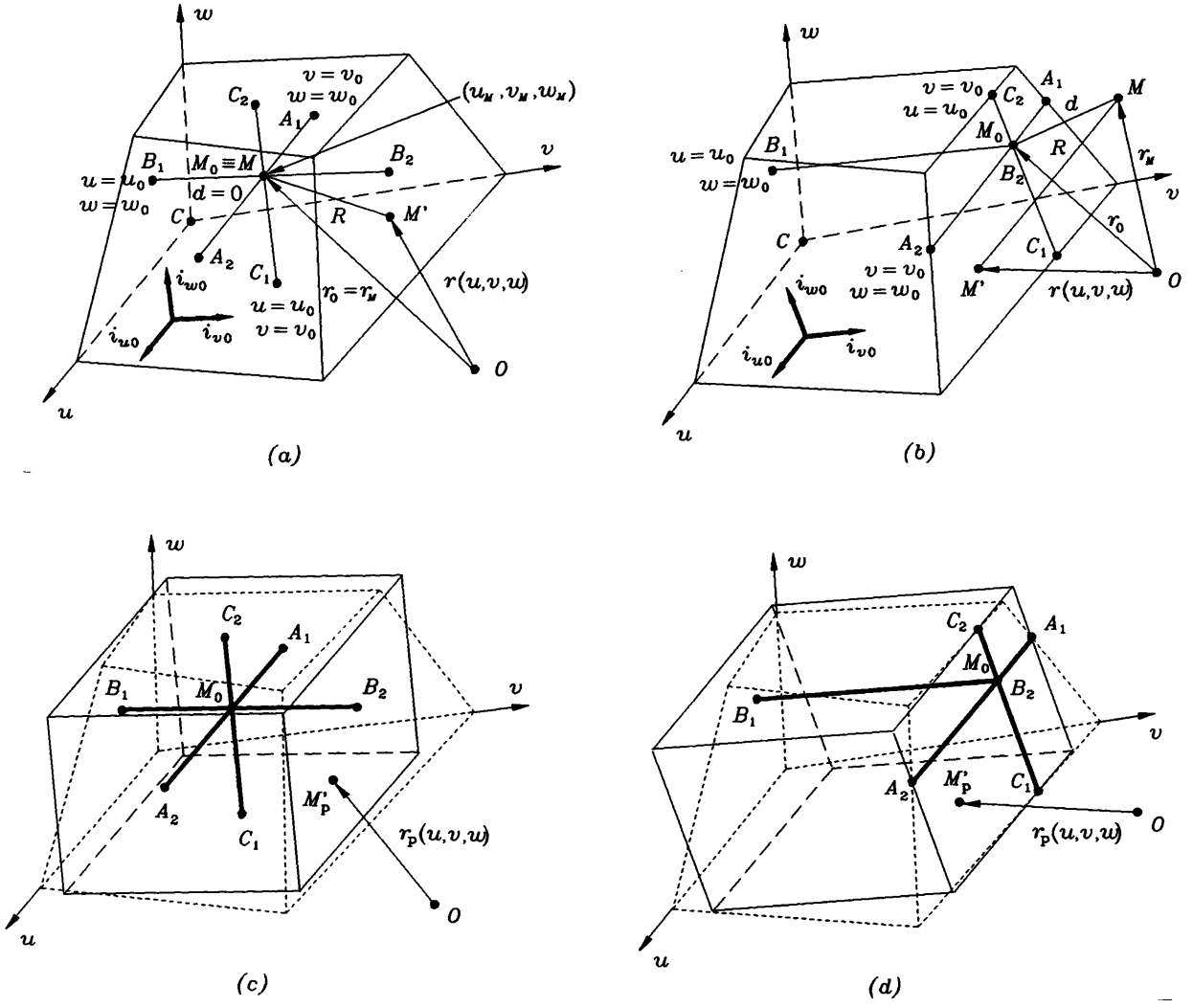

Figure 3. (a) Field point M inside trilinear hexahedron (which contains the source point, M') or on its surface; (b) field point outside hexahedron; (c) parallelepiped for extraction of singularity in case (a); (d) parallelepiped for extraction of quasisingularity in case (b)

$$P_{ijk} = \frac{1}{4\pi}\left[\int_{u_1}^{u_2}\int_{v_1}^{v_2}\int_{w_1}^{w_2}\left(u^i v^j w^k \frac{e^{-j\beta_0 R}}{R} - u_0^i v_0^j w_0^k \cos\beta_0 d \frac{1}{R_p}\right) du\,dv\,dw + u_0^i v_0^j w_0^k \cos\beta_0 d \int_{u_1}^{u_2}\int_{v_1}^{v_2}\int_{w_1}^{w_2}\frac{1}{R_p}\,du\,dv\,dw\right] \tag{25}$$

where $R_p = |\mathbf{r}_M - \mathbf{r}_p(u,v,w)|$, and $\mathbf{r}_p$ is the position vector of the point M_p'. In the above equation, the integrand of the first integral is well behaved in the vicinity of the point (u_0,v_0,w_0) and can be integrated numerically with ease. Note that this integral represents a triple integral over the domain $u_1 \le u \le u_2,\ v_1 \le v \le v_2,\ w_1 \le w \le w_2$, which, however, represents the domain of both the trilinear hexahedron and the parallelepiped.

Let us denote the second integral in equation (25) by P_0'. It is a simple matter to prove that

$$P_0' = P_0/K_0,\ K_0 = K(u_0,v_0,w_0),\ P_0 = \int_{V_p}\frac{1}{R_p}\,dV_p \tag{26}$$

where V_p is the volume of the parallelepiped. The integral P_0 can be integrated analytically.[8]

Equation (25) can also be transformed into the following form:

$$P_{ijk} = (P_{ijk})_{\text{numerical}} + \frac{u_0^i v_0^j w_0^k \cos\beta_0 d}{4\pi}\left[(P_0')_{\text{analytical}} - (P_0')_{\text{numerical}}\right] \tag{27}$$

which explains that, actually, the difference between the exact (analytical) and approximate (numerical) solution for the integral P_0' over the domain of the corresponding parallelepiped represents a correction for the approximate solution of the integral P_{ijk} over the domain of the trilinear hexahedron.

To enhance accuracy of numerical integration, if (quasi)singularity is extracted we shall subdivide the domain of triple numerical integration, $u_1 \le u \le u_2,\ v_1 \le v \le v_2,\ w_1 \le w \le w_2$, into 2^l integration subdomains by means of co-ordinate surfaces $u = u_0,\ v = v_0$ and $w = w_0$. If the point M_0 is inside the hexahedron, $l = 3$. If it is on one of the sides, $l = 2$. Finally, if it is along the edge of the hexahedron, $l = 1$. When M_0 coincides with a vertex of the hexahedron, the division into subdomains is skipped ($l = 0$).

The basic 2D potential integral, $Q_{jk}^{(l)}$, over the surface of the bilinear quadrilateral, given in (18), is integrated in a similar manner.

3.1. *Optimization of the algorithm for multiple numerical integration*

Based on the Gauss–Legendre single-integral integration formula, the integration formula for the triple integrals P_{ijk} has the form

$$(P_{ijk})_{\text{numerical}} = \sum_{m=1}^{N_{Gu}}\sum_{n=1}^{N_{Gv}}\sum_{l=1}^{N_{Gw}} A_m A_n A_l u_m^i v_n^j w_l^k g[R(u_m,v_n,w_l)]$$
$$i = 0, 1, \ldots, N_u + 1,\ j = 0, 1, \ldots, N_v + 1,\ k = 0, 1, \ldots, N_w + 1 \tag{28}$$

In this expression, N_u, N_v and N_w are the adopted degrees of the polynomial approximation for current in the trilinear hexahedron considered, N_{Gu}, N_{Gv} and N_{Gw} are degrees, u_m, v_n and w_l are arguments (zeros of the Legendre polynomials) and A_m, A_n and A_l are weights of the corresponding Gauss–Legendre integration formulas, respectively.

Equation (28) is also the algorithm which can be used directly as the basis for the evaluation of the considered sequence of triple integrals. Such a program, however, would require unnecessarily long computing time, since all indicated operations would be performed for all values of the summation indices m, n and l, as well as for all values of the indices i, j and k of the power basis functions. Fortunately, this can be avoided, because (28) can be transformed into

$$[P]_{\text{numerical}} = \left\{ [P]^{***}: \sum_{m=1}^{N_{Gu}} A_m \left| \begin{matrix}\text{comput.}\\ \text{of}\\ b_{pq}(u_m)\end{matrix} \right| \left[[H]^{**}: \sum_{n=1}^{N_{Gv}} A_n \left| \begin{matrix}\text{computat.}\\ \text{of}\\ a_p(v_n)\end{matrix} \right| \right.\right.$$

$$\left([G]^{*}: \sum_{l=1}^{N_{Gw}} A_l \left| \begin{matrix}\text{computat.}\\ \text{of}\\ R^2(w_l)\end{matrix} \right| g(R) \left| \begin{matrix} W_k = w_l\ W_{k-1} \\ k=1,\ \ldots,\ N_{w1} \\ W_0 = 1 \end{matrix} \right| W_k \right) \left| \begin{matrix} V_j = v_n\ V_{j-1} \\ j=1,\ \ldots,\ N_{v1} \\ V_0 = 1 \end{matrix} \right| V_j \left. \right]$$

$$\left. \left| \begin{matrix} U_i = u_m\ U_{i-1} \\ i=1,\ \ldots,\ N_{u1} \\ U_0 = 1 \end{matrix} \right| U_i \right\} \tag{29}$$

where * is evaluation of temp. vector G_k ($k = 0, \ldots, N_{w1}$), ** is evaluation of temp. vector H_{jk} ($j = 0, \ldots, N_{v1}$, $k = 0, \ldots, N_{w1}$) and *** is evaluation of final results. $N_{u1} = N_u + 1$, $N_{v1} = N_v + 1$, $N_{w1} = N_w + 1$, and the functions $R^2(w)$, $a_p(v)$ and $b_{pq}(u)$ are defined in (20)–(23). The algorithm summarized in (29) contains a number of numerical details[5] which will not be elaborated here. The corresponding computer program is significantly more rapid than that according to (28): the necessary CPU time is usually reduced for more than an order of magnitude. This is of extreme importance, since, during a complete analysis of a given dielectric scatterer, the basic potential integrals need to be evaluated many times.

The test (outer) integration in the Galerkin integrals is performed only numerically, using the optimized algorithm proposed in this Section. In doing this, if the integrals S in (23) are considered, it is necessary to replace $g(R)$ by $P_{i_n j_n k_n}$, which, at any integration point, should be evaluated for all necessary values of the indices i_n, j_n and k_n simultaneously. In addition to this temporary vector $P_{i_n j_n k_n}$, in analogy with the vectors G_k and H_{jk} in (29), it is necessary to use also temporary vectors $G_{k_m i_n j_n k_n}$ and $H_{j_m k_m i_n j_n k_n}$. Of course, the proposed optimization of the test integration in the Galerkin integrals is also of exceptional significance for efficiency of the entire analysis method.

Finally, for reference, in the following Section, let us label the orders of the Gauss–Legendre integration formula of the basic potential integrals P and Q [equations (17) and (18)] by $N_{Gu}^{(b)}$, $N_{Gv}^{(b)}$ and $N_{Gw}^{(b)}$, and the orders of the outer (testing) integration in the Galerkin integrals [equations (23) and (24)] by $N_{Gu}^{(t)}$, $N_{Gv}^{(t)}$ and $N_{Gw}^{(t)}$. Of course, the parameters $N_G^{(b)}$ and $N_G^{(t)}$ are adopted individually for all the hexahedrons used for the approximation of the scatterer.

4. NUMERICAL RESULTS AND DISCUSSION

We now illustrate the accuracy and efficiency of the proposed optimized entire-domain method for the analysis of 3D dielectric scatterers on actual numerical examples. All results were obtained on a PC-486/66 MHz (8 MB DRAM) using Fortran 77 (Lahey F77L-EM/32).

4.1. *Numerical results for basic potential integrals*

Consider first the accuracy and efficiency of the proposed procedure of combined numerical/analytical integration of the volume potential integrals P_{ijk}, defined in (17). Consider a highly twisted trilinear hexahedron. Let its vertices be defined by (see Figure 1): $\mathbf{r}_{111} = (-0{\cdot}5\lambda_0;\ -0{\cdot}5\lambda_0;\ -0{\cdot}5\lambda_0)$, $\mathbf{r}_{112} = (-0{\cdot}5\lambda_0;\ -0{\cdot}5\lambda_0;\ 0{\cdot}5\lambda_0)$, $\mathbf{r}_{121} = (-0{\cdot}7\lambda_0;\ 0{\cdot}7\lambda_0;\ -0{\cdot}7\lambda_0)$, $\mathbf{r}_{122} = (-0{\cdot}4\lambda_0;\ 0{\cdot}4\lambda_0;\ 0{\cdot}6\lambda_0)$, $\mathbf{r}_{211} = (0{\cdot}5\lambda_0;\ -0{\cdot}5\lambda_0;\ -0{\cdot}5\lambda_0)$, $\mathbf{r}_{212} = (0{\cdot}3\lambda_0;\ -0{\cdot}3\lambda_0;\ 0{\cdot}5\lambda_0)$, $\mathbf{r}_{221} = (0{\cdot}8\lambda_0;\ 0{\cdot}5\lambda_0;\ -0{\cdot}5\lambda_0)$, $\mathbf{r}_{222} = (0{\cdot}8\lambda_0;\ 0{\cdot}8\lambda_0;\ 0{\cdot}8\lambda_0)$, where λ_0 is the free-space wavelength. Assume that the

Table I. Relative error of $\mathrm{Re}\{P_{000}\}$ vs. the integration parameters, for a field point (a) inside a trilinear hexahedron and (b) outside it. For details please see text

Integration parameters			(a)	(b)
$N_G^{(b)} = 24$,	$N_{seg} = 1$,	without extraction	$6{\cdot}517 \times 10^{-3}$	$-7{\cdot}001 \times 10^{-3}$
$N_G^{(b)} = 5$,	$N_{seg} = 2$,	without extraction	$-2{\cdot}388 \times 10^{-3}$	$-1{\cdot}731 \times 10^{-3}$
$N_G^{(b)} = 24$,	$N_{seg} = 2$,	without extraction	$2{\cdot}519 \times 10^{-5}$	$-9{\cdot}497 \times 10^{-4}$
$N_G^{(b)} = 5$,	$N_{seg} = 2$,	with extraction	$2{\cdot}147 \times 10^{-6}$	$8{\cdot}380 \times 10^{-6}$

boundary parametric co-ordinates are $u_1 = v_1 = w_1 = -1$ and $u_2 = v_2 = w_2 = 1$, and that $N_{Gu}^{(b)} = N_{Gv}^{(b)} = N_{Gw}^{(b)} = N_G^{(b)}$.

Table I shows relative errors in the real part of the integral P_{000} (its imaginary part is not singular), vs. the integration parameters. The reference ('exact') values of the integrals were those obtained with $N_G^{(b)} = 24$, $N_{seg} = 2$ and the extraction of (quasi)singularity, where N_{seg} is the number of subsegments of the integration [see the first paragraph following (27)]. The results are presented for a field point M situated (a) inside the hexahedron (a singular point, $d = 0$), defined in local parametric co-ordinates as $u_M = v_M = w_M = 0{\cdot}4$ [see Figure 3(a)], and (b) outside the hexahedron, but very close to its side defined by $v = v_2$ [see Figure 3(b)]. In case (b) it was adopted that $\mathbf{r}_M = (0;\ 0{\cdot}5925\lambda_0;\ 0)$, which corresponds to the co-ordinates $u_0 = -0{\cdot}178701$, $v_0 = 1$ and $w_0 = -0{\cdot}0494324$ of the point M_0 and to the distance from the closest hexahedron side $d = R_{min} = 0{\cdot}000110206\lambda_0$. This means that the integral has a very pronounced quasisingularity. The results were obtained with single-precision arithmetic, i.e. with six significant digits.

We see from Table I that excellent results are obtained (having in mind the single-precision arithmetic used) with quite a low order of the Gauss–Legendre integration formula ($N_G^{(b)} = 5$), but only if the procedure of extraction of (quasi)singularity is performed. In other words, this procedure enables considerable reduction in the order $N_G^{(b)}$. As a consequence, the resulting CPU time for the problem analysis appears to be very much reduced (usually for two orders of magnitude) than in the case without the extraction procedure.

Similar results are obtained also for the integrals $Q_{jk}^{(l)}$ in (18), where the domain of integration represents the surface of a bilinear quadrilateral (Figure 2).[5]

4.2. *Rod-like dielectric scatterer*: *convergence analysis*

We next analyse convergence of the current distribution and of the bistatic scattering cross-section vs. the parameters of the method for a rod-like dielectric scatterer.

Assume that for the scatterer sketched in Figure 4 $a = \lambda_0/10$, $l = 2\lambda_0 = 20{\cdot}8\lambda_d$ (λ_d is the wavelength in the dielectric) and $\epsilon_{er} = \epsilon_r - j\sigma/(\omega\epsilon_0) = 75 - j119{\cdot}83$ (an electrically long rod-like scatterer made of a dielectric of high relative permittivity and with high losses). Let the incident

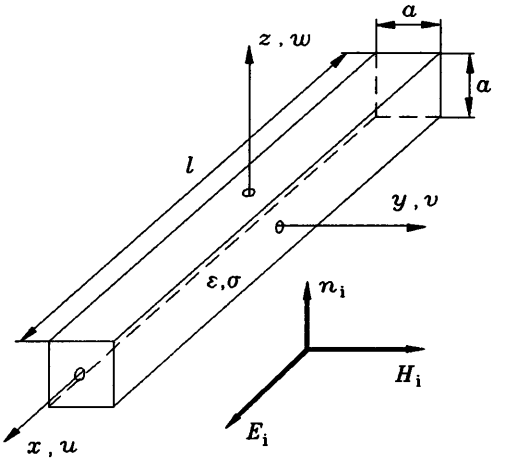

Figure 4. Rod-like homogeneous dielectric scatterer of square cross-section

field be that of a plane wave, with the electric field vector $\mathbf{E}_i = 1 \exp(-j\beta_0 z)\ \mathbf{i}_x$V/m. According to the present method, the scatterer in Figure 4 is modelled by a single trilinear hexahedron. Figure 5(a) shows the results for the distribution of the current density vector, **J**, along the long scatterer axis, and in Figure 5(b) the results for the normalized bistatic cross-section of the scatterer, $S_{\text{bist}}/\lambda_0^2$, in the plane $\phi = 0$ (the *E*-plane), for different orders N_u of the current approximation along the parametric *u*-axis, with $N_v = N_w = 1$. In all the cases the following values for the parameters of integration were adopted: $N_{Gu}^{(t)} = 12$, $N_{Gv}^{(t)} = N_{Gw}^{(t)} = 4$, $N_{Gu}^{(b)} = 12$ and $N_{Gv}^{(b)} = N_{Gw}^{(b)} = 4$. The Figures indicate a rapid convergence of the results with increasing degree N_u of the approximation. We see that the results are stabilized completely with $N_u = 8$. Note again that the scatterer is electrically rather long ($l = 20{\cdot}8\lambda_d$).

Let us now analyse the convergence of the current density vector as a function of the parameters of integration for the rod-like scatterer considered. The degrees of approximation were adopted

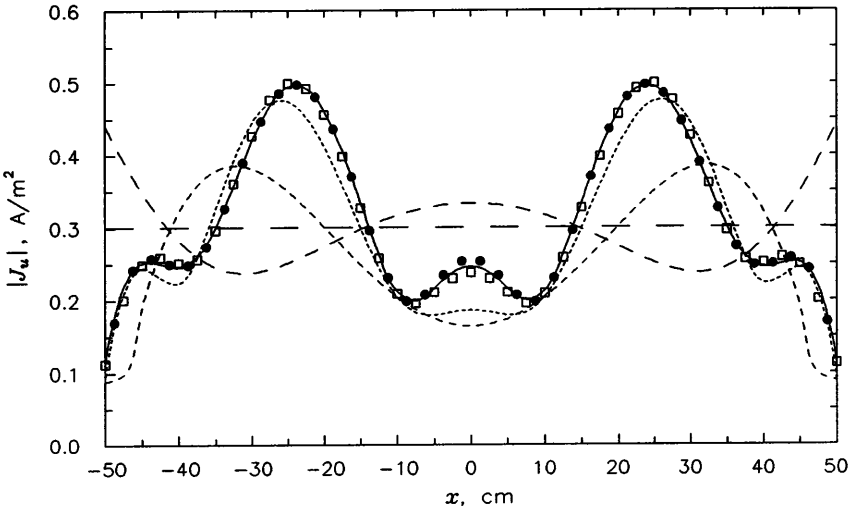

(a)

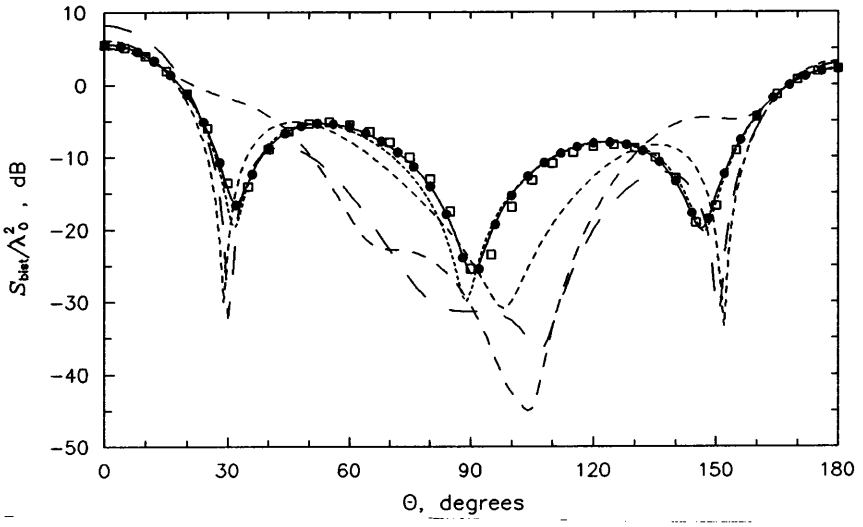

(b)

Figure 5. Convergence of results with increasing degree of approximation, N_u, for scatterer from Figure 4 [$\epsilon_{er} = 75 - j119{\cdot}83$, $l = 2\lambda_0 = 20{\cdot}8\lambda_d = 100$ cm, $a = \lambda_0/10$, $(E_i)_0 = 1$ V/m]: (a) intensity of total current density, $|\mathbf{J}_u|$, along *u*-axis; (b) normalized bistatic cross-section of the scatterer, 10 $\log(S_{\text{bist}}/\lambda_0^2)$, in *E*-plane ($\phi = 0$) —— $N_u = 1$; – – – $N_u = 2$; ----- $N_u = 4$; ···· $N_u = 6$; □ □ □ $N_u = 8$; • • • $N_u = 10$; ———— $N_u = 12$

resulting in a stable solution, i.e. $N_u = 8$ and $N_v = N_w = 1$ (see Figure 5). Figure 6(a) shows the results obtained for different orders of the Gauss–Legendre integration formula $N_{Gu}^{(t)}$, $N_{Gv}^{(t)}$ and $N_{Gw}^{(t)}$, relating to the test procedure, with other integration parameters kept constant, i.e. $N_{Gu}^{(b)} = 12$ and $N_{Gv}^{(b)} = N_{Gw}^{(b)} = 4$. On the other hand, if we adopt fixed $N_{Gu}^{(t)} = 12$ and $N_{Gv}^{(t)} = N_{Gw}^{(t)} = 4$, and consider as variables the orders of the Gauss–Legendre integration formula $N_{Gu}^{(b)}$, $N_{Gv}^{(b)}$ and $N_{Gw}^{(b)}$, relating to the integration of the basic potential integrals, P and Q, curves in Figure 6(b) are obtained instead.

We see that the results in Figure 6(a) are entirely in agreement with the conclusion that the Galerkin method is well defined only if the number of the integration points per co-ordinate in the test integration is not less than the number of unknowns in that co-ordinate.[7] In our case, this means that the theoretically minimal orders of the Gauss–Legendre integration formula are

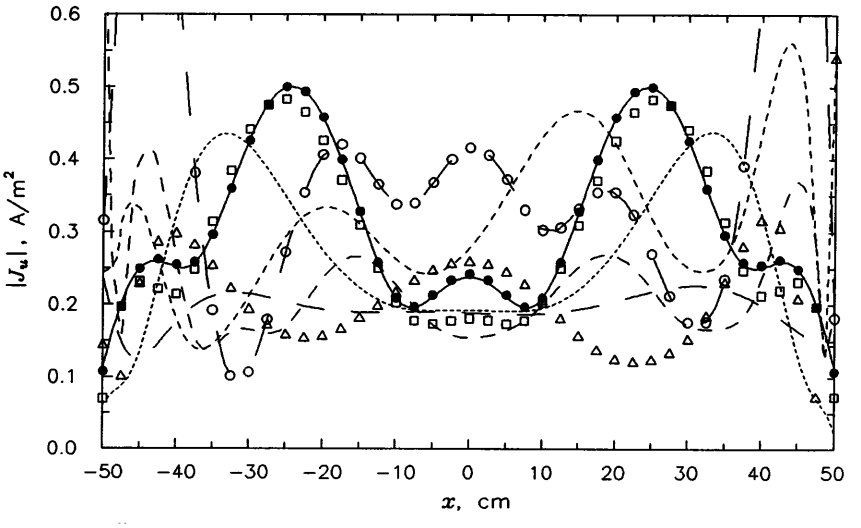

(a)

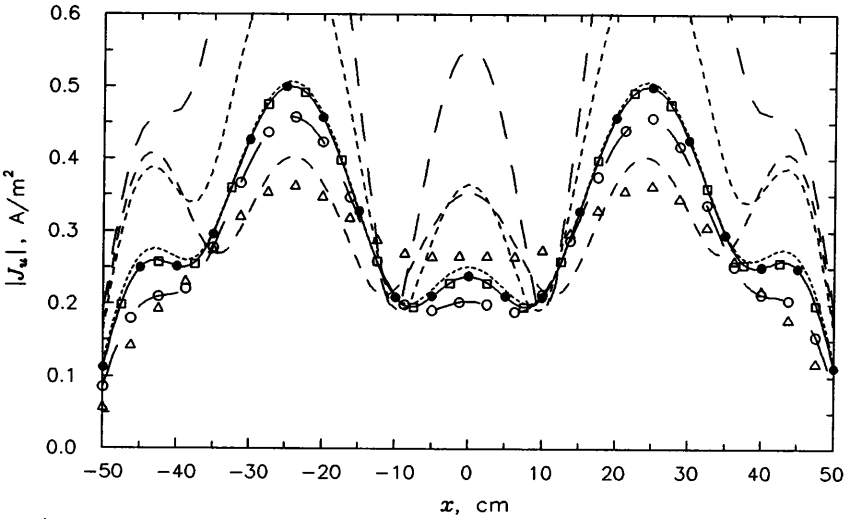

(b)

Figure 6. Distribution of total current density, $|\mathbf{J}_u|$, along u-axis of the scatterer in Figure 4 [$\epsilon_{er} = 75 - j119{\cdot}83$, $l = 2\lambda_0 = 20{\cdot}8\lambda_d = 100$ cm, $a = \lambda_0/10$, $(E_i)_0 = 1$ V/m], for different orders of Gauss–Legendre integration formula (N_{Gu},N_{Gv},N_{Gw}), referring to (a) test procedure and (b) integration of the basic integrals, with $N_u = 8$ and $N_v = N_w = 1$ — — (2,2,2), △ △ △ (3,2,2); – – – (4,2,2); ---- (5,2,2); ○ —— (6,2,2); ------ (7,2,2); □ □ □ (8,2,2); • • • (9,2,2); ———— (12,4,4)

$$N_{Gu}^{(t)} = N_u + 1,\ N_{Gv}^{(t)} = N_v + 1,\ N_{Gw}^{(t)} = N_w + 1 \tag{30}$$

With the present method it was found that the orders defined in the above equations, which are the lowest possible, already result in stable solution, which is also clear from Figure 6(a). (Note that this is in contrast to the specific Galerkin method for the analysis of metallic scatterers,[9] where a significantly higher order of Gauss–Legendre integration formulas than the minimal were found to be necessary.) Such low orders of the Gauss–Legendre formula make the analysis of dielectric scatterers quite rapid, practically the same as if point-matching is used instead of Galerkin testing, in spite of multiple integration required in the latter. Of course, this is due also to the optimized test integrations in the Galerkin integrals.

Figure 6(b) shows that practically the same results are obtained for all values of the order $N_{Gu}^{(b)}$ which satisfy the condition $N_{Gu}^{(b)} \geq N_u - 1$. Based on this conclusion, as well as on many other numerical experiments, it was indeed found that the choice of the orders of Gauss–Legendre integration formula following the rules

$$N_{Gu}^{(b)} = N_u + 1,\ N_{Gv}^{(b)} = N_v + 1,\ N_{Gw}^{(b)} = N_w + 1 \tag{31}$$

in all volume elements of the model, resulted in stable results in practically all applications of the method.

Finally, on the basis of the above examples it can be concluded that, in the analysis of dielectric scatterers proposed in this paper, it is sufficient to adopt quite low values for the degrees, N, of the polynomial approximation of current and the orders of the Gauss–Legendre integration formulas, ($N_G^{(t)}$ and $N_G^{(b)}$). Such favourable numerical performances of the Galerkin method used in this paper are the result of both the flexibility of the adopted polynomial approximation of current-density vector **J**, and of the accuracy and efficiency of the proposed procedure for the evaluation of the Galerkin generalized impedances. When compared with the existing methods for the analysis of dielectric scatterers (which, as mentioned, are all of subdomain type), the proposed Galerkin method requires much fewer unknowns for a given problem (for one, and even for two, orders of magnitude[5]).

4.3. *Cubical dielectric scatterer*: *CPU time*

The final check of the efficiency of the proposed method as a whole is the necessary CPU time. In this Section we analyse the dependence of individual parts of the CPU time on the parameters of the current approximation and integration by considering a homogeneous dielectric cube of side length $a = \lambda_0$, situated in the field of a plane wave. In all cases we adopt $N_u = N_v = N_w = N$, $N_{Gu}^{(t)} = N_{Gv}^{(t)} = N_{Gw}^{(t)} = N_G^{(t)}$ and $N_{Gu}^{(b)} = N_{Gv}^{(b)} = N_{Gw}^{(b)} = N_G^{(b)}$ (the cube is modelled by a single volume element).

Table II shows the CPU time necessary for the evaluation of the system matrix (the Galerkin generalized impedances) and of the vector of free terms (Galerkin generalized voltages), T_{mat}, for different values of the parameters N, $N_G^{(t)}$ and $N_G^{(b)}$, with $N_G^{(t)} = N_G^{(b)} = N_G$. Also given in the Table are the values for the total number of unknowns, N_{unk}, corresponding to the cases considered.

Inspecting these data it is possible to conclude that, if we increase the degree, N, of the polynomial, i.e. the total number of unknowns, for a constant order of the Gauss–Legendre integration formula, N_G (left part of the table), the time T_{mat} increases much slower than the function N_{unk}^2, where $N_{unk}^2 = 9(N+1)^6$ represents the number of the elements of the system matrix.

Table II. Dependence of the CPU time necessary for evaluating the system matrices, T_{mat}, on the parameters of the method, in the case of the analysis of a dielectric cube in the field of a plane wave

N	N_{unk}	$N_G^{(t)}$	$N_G^{(b)}$	T_{mat}, s	N	N_{unk}	$N_G^{(t)}$	$N_G^{(b)}$	T_{mat}, s
1	24	6	6	44·43	4	375	3	3	19·50
2	81	6	6	51·36	4	375	4	4	30·60
3	192	6	6	64·09	4	375	5	5	53·55
4	375	6	6	96·67	4	375	6	6	96·67
5	648	6	6	166·53	4	375	7	7	175·43

We also see that, by increasing N_G and keeping N constant (right part of the table), the time T_{mat} increases much slower than the function $(N_G)_{3D/3D} = N_G^3 \times (2N_G)^3 = 8N_G^6$. [This function is proportional to the total number of operations necessary for performing the sixfold integration of the 3D/3D Galerkin integrals, $S_{i_m j_m k_m i_n j_n k_n}$, defined in (23), if all the operations were performed inside all the six summation signs. $2N_G$ stands instead of N_G, because all inner volume integrations are performed by extracting the singularity, which implies subdivision into two subsegments in integrating along all three co-ordinates.] This favourable dependence of T_{mat} on N and N_G is the consequence of the adopted efficient, non-redundant evaluation of the Galerkin generalized impedances.

Table III gives data for the time T_{mat}, as well as for the computing time T_{sys} necessary for the solution of the corresponding system of linear algebraic equations by the Gaussian elimination method, for different degrees of N of the polynomials, with the orders $N_G^{(t)}$ and $N_G^{(b)}$ of the Gauss–Legendre integration formula given in (30) and (31). As we have seen in Subsection 4.2, such a choice of the integration parameters ensures sufficiently accurate solution, provided that adequate degrees of the approximation for current are adopted.

Based on the data shown, it is possible to conclude that the dependence $T_{mat}(N_{unk})$ is relatively close to $T_{mat} = A N_{unk}^2$ (A is a constant), standard also for subdomain solutions obtained by the method of moments. On the other hand, we see that the time T_{sys} very nearly satisfies the equation $T_{sys} = B N_{unk}^3$ (B is a constant), as it should.

As a natural consequence of much smaller number of unknowns and of the efficient evaluation of the Galerkin generalized impedances explained, it has been found by numerous numerical experiments that the proposed entire-domain method in all cases was highly superior when compared with the available (subdomain) methods,[5] as far as the total computing time is concerned.

4.4. *Spherical dielectric scatterer*: *comparison with the exact solution*

This last example is aimed at illustrating the flexibility of the adopted geometrical model, and the accuracy and efficiency of the proposed procedure for the evaluation of the Galerkin generalized impedances for a body approximated by relatively large number of trilinear hexahedrons. To that end a spherical scatterer is very convenient, because the exact solution in that case is available.

Consider a homogeneous sphere made of a perfect dielectric of relative permittivity $\epsilon_r = 2$. The origin of the global Cartesian x-y-z co-ordinate system is adopted to be at the centre of the sphere. Assume that the sphere is excited by a linearly polarized plane wave with $\mathbf{E}_i = 1 \exp(-j\beta_0 z)\ \mathbf{i}_x$ V/m. Let the radius of the sphere be given by $\beta_0 a = 2{\cdot}744$ ($2a = 1{\cdot}235\lambda_d$). It turns out that this is a resonant scatterer.[10]

We approximate the sphere by $3 \times 3 \times 3 = 27$ trilinear hexahedrons, with $6 \times (3 \times 3) = 54$ (curved and plane) bilinear quadrilaterals approximating its surface, as in Figure 7. The volume of the model equals the volume of the sphere. Note that the surface of the sphere is approximated fairly accurately with quite a small number (27) of geometrical elements. The first degree of the polynomial approximation was adopted in all the 27 hexahedrons ($N_u = N_v = N_w = 1$), so that this, essentially, was the subdomain form of the Galerkin method. The number of unknowns was additionally reduced by automatically enforcing the continuity condition for the normal component of the vector $\epsilon_e \mathbf{E}$ on adjacent surfaces of hexahedrons[5] (namely, with this, the number of basis functions along each Cartesian co-ordinate was reduced from 6 to 4). The parameters of integration

Table III. Dependence of T_{mat} and T_{sys} on the degree N of the polynomial, for the analysis of a dielectric cube in the field of a plane wave. The parameters of integration, $N_G^{(t)}$ and $N_G^{(b)}$, are adopted as in (30) and (31)

N	N_{unk}	$N_G^{(t)}$	$N_G^{(b)}$	T_{mat}, s	T_{sys}, s
1	24	2	2	1·15	0·06
2	81	3	3	4·23	0·43
3	192	4	4	15·22	6·15
4	375	5	5	51·19	54·32
5	648	6	6	166·53	315·60

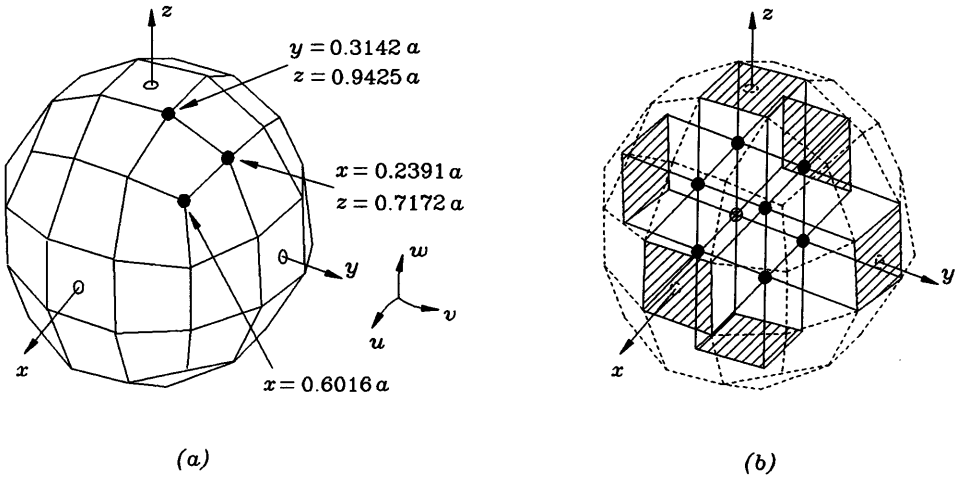

Figure 7. Approximation of a homogeneous dielectric sphere by 27 trilinear hexahedrons. The sphere surface was first approximated by 54 bilinear quadrilaterals (a), and then its volume subdivided into 27 hexahedrons (b)

were adopted in accordance with (30) and (31). Symmetry and antisymmetry were partly used. The resulting number of unknowns was $N_{\text{unk}} = 208$, and the total computing time $T_{\text{tot}} = 134{\cdot}25$ s.

Figure 8 shows the results for the bistatic scattering cross-section of the sphere, $S_{\text{bist}}/\lambda_0^2$, in two characteristic planes. The results obtained by the proposed method are compared with the exact results in the form of a Mie series,[10] as well as with those obtained by the subdomain hybrid symmetric FEM/MOM method (for BOR).[10] Excellent agreement is seen between the three sets of results. However, the number of basis functions per λ_d required by the method from Reference 10 was 15, while with the method proposed in this paper it was as small as about 3.

5. CONCLUSION

The paper describes a procedure for evaluating generalized Galerkin impedances in the moment-method analysis of arbitrary 3D dielectric scatterers approximated by trilinear hexahedrons with entire-domain polynomial approximation of volume current. The procedure consists in two steps. In the first step, the expressions for the impedances are derived which are particularly convenient for numerical evaluation. In the second step, efficient evaluation is performed of multiple integrals representing these impedances and of the entire impedance matrix.

Numerical examples are given of the implementation of the combined analytical/numerical

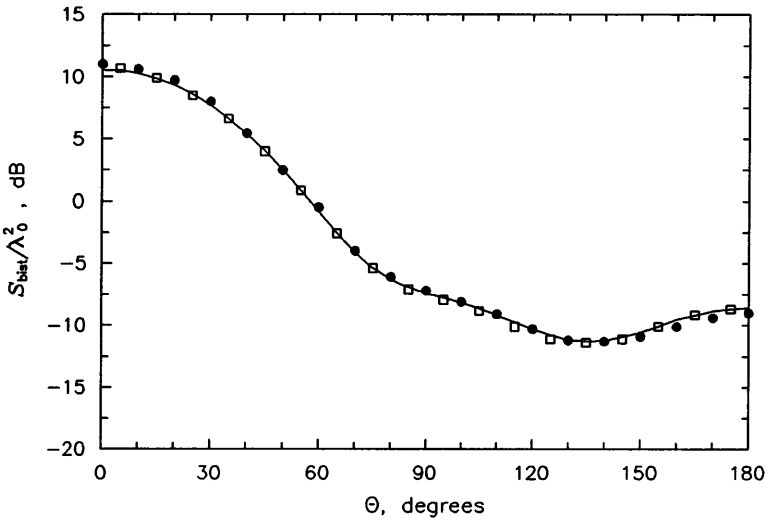

Figure 8. Normalized bistatic cross-section, $10\log(S_{\text{bist}}/\lambda_0^2)$, of a homogeneous lossless resonant dielectric sphere [$\beta_0 a = 2{\cdot}744$, $\epsilon_r = 2$, $\mathbf{E}_i = 1\exp(-j\beta_0 z)\,\mathbf{i}_x$ (V/m)], in plane $\phi = 0$ ——— this method; • • • analytical solution in the form of Mie series;[10] □ □ □ symmetric FEM/MOM for BOR with 15 basis functions/λ_d (Reference 10)

method of integration of basic potential integrals illustrating its efficiency and accuracy. Examples of stable and rapid convergence of the results with the increasing degree of approximation is also illustrated for both inner (near) and far fields. A relatively slow increase in CPU time is demonstrated with the increase of the degree of polynomial approximation of volume current and the parameters of integration of the Galerkin integrals. As a specific example, the method is used for the analysis of a spherical dielectric scatterer, for which an analytic solution is available, to illustrate the accuracy and efficiency of the entire method.

In the authors' opinion, entire-domain analysis of dielectric scatterers is greatly superior to subdomain analysis, concerning the number of unknowns, memory requirement and CPU time. However, these advantages become evident and convincing only if the entire-domain approach is carefully planned and optimized. This paper shows how this can be done in the most difficult and critical part of the Galerkin-type analysis of 3D dielectric scatterers, the evaluation of the Galerkin generalized impedances. It is hoped, however, that some of the procedures outlined in the paper may be of interest in any type of optimized entire-domain method-of-moment analysis of electromagnetic systems.

REFERENCES

1. D. H. Schaubert, D. R. Wilton and A. W. Glisson, 'A tetrahedral modeling method for electromagnetic scattering by arbitrarily shaped inhomogeneous dielectric bodies', *IEEE Trans*., **AP-32** (1), 77–85 (1984).
2. T. K. Sarkar, E. Arvas and S. Ponnapalli, 'Electromagnetic scattering from dielectric bodies', *IEEE Trans*., **AP-37** (5), 673–676 (1989).
3. P. Zwamborn and P. M. van den Berg, 'The three-dimensional weak form of the conjugate gradient FFT method for solving scattering problems', *IEEE Trans*., **MTT-40** (9), 1757–1766 (1992).
4. B. D. Popović and B. M. Notaroš, 'Entire-domain polynomial approximation of volume currents in the analysis of dielectric scatterers', *IEE Proc., Microw. Antennas Propag*., **142** (3), 207–212 (1995).
5. B. M. Notaroš, *Numerical analysis of dielectric bodies of arbitrary shape and inhomogeneity in the electromagnetic field* (in Serbian), D.Sc. thesis, Department of Electrical Engineering, University of Belgrade, 1995.
6. R. F. Harrington, *Field Computation by Moment Methods*, Macmillan, New York, 1968.
7. B. D. Popović and B. M. Kolundžija, 'Analysis of metallic antennas and scatterers', *IEE Electromagnetic Wave Series, No. 38*, London, 1994.
8. D. R. Wilton, S. M. Rao, A. W. Glisson, D. H. Schaubert, O. M. Al-Bundak and C. M. Butler, 'Potential integrals for uniform and linear source distributions on polygonal and polyhedral domains', *IEEE Trans*., **AP-32** (3), 276–281 (1984).
9. B. M. Kolundžija, *Electromagnetic modelling of composite wire and plate structures* (in Serbian), D.Sc. thesis, Department of Electrical Engineering, University of Belgrade, 1990.
10. D. J. Hoppe, L. W. Epp and J.-F. Lee, 'A hybrid symmetric FEM/MOM formulation applied to scattering by inhomogeneous bodies of revolution', *IEEE Trans*., **AP-42** (6), 798–805 (1994).

Authors' biographies:

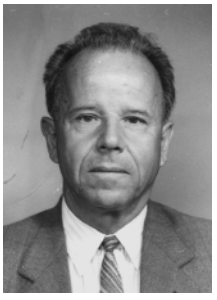

Branko D. Popović, a member of the Serbian Academy of Sciences and Arts and a Fellow of the IEE, is a Professor of Electrical Engineering at the University of Belgrade, Yugoslavia. He is the author or coauthor of numerous papers on antennas and applied electromagnetics, of a number of textbooks, and of three monographs on the analysis and CAD of wire and metallic antennas and scatterers. He was awarded the *Heinrich Hertz Premium* of the British IERE (1974), the *James Clerk Maxwell Premium* of the IEE (1985), the Yugoslav *Nikola Tesla Premium* (1985) and a number of other Yugoslav awards.

Branislav M. Notaroš was born in 1965 in Zrenjanin, Yugoslavia. He received B.Sc., M.Sc. and Ph.D. degrees in electrical engineering from the University of Belgrade, Yugoslavia, in 1988, 1992 and 1995, respectively. He was awarded the Belgrade Trade Association Prize for the best M.Sc. thesis in 1992. Dr. Notaroš is an Assistant Professor of Electromagnetics at the Department of EE, University of Belgrade. He is a coauthor of several papers, published in periodicals or presented at conferences. His research interests are in numerical analysis of metallic and/or dielectric antennas and scatterers.

